



Article

# A Series of Zinc Mononuclear Complexes with Imidoyl Amidine Ligands: Syntheses, Crystal Structures, and Photoluminescence Properties

Mart Ruben Nijhuis <sup>1</sup>, Zaina Yamba <sup>1</sup>, Egor Novikov <sup>1</sup>, Marina S. Fonari <sup>1,2</sup>, Tatiana V. Timofeeva <sup>1,\*</sup> and Raúl Castañeda <sup>1,\*</sup>

- Department of Chemistry, New Mexico Highlands University, Las Vegas, NM 87701, USA; enovikov@live.nmhu.edu (E.N.); fonari.xray@gmail.com (M.S.F.)
- Institute of Applied Physics, Moldova State University, Academy Str. 5, MD2028 Chisinau, Moldova
- \* Correspondence: tvtimofeeva@nmhu.edu (T.V.T.); lrcastaneda@ucsb.edu (R.C.)

Abstract: Three amidine-based ligands were used in the crystal design of a series of mononuclear Zn(II) complexes. Interaction of zinc chloride, ZnCl<sub>2</sub>, with N-2-pyridylimidoyl-2-pyridylamidine (Py<sub>2</sub>ImAm) resulted in complexes [Zn(Py<sub>2</sub>ImAm)<sub>2</sub>] (1) and [ZnCl<sub>2</sub>(Py<sub>2</sub>ImAm)] (2). In [Zn(Py<sub>2</sub>ImAm)<sub>2</sub>]  $(1, monoclinic, P2_1/c)$ , the metal ion was coordinated with the bidentate pocket of the anionic form of  $Py_2ImAm$ , while in  $[ZnCl_2(Py_2ImAm)]$  (2, monoclinic,  $P2_1/n$ ), the tridentate coordination to a neutral Py<sub>2</sub>ImAm was completed by two chloride anions. This structural variation was achieved by a pH-controlling strategy using the weak base triethylamine (TEA). Otherwise, three ionic complexes were obtained with 2-amidinopyridine (PyAm) and Zinc(II), [ZnCl(PyAm)<sub>2</sub>]Cl (3, triclinic, P-1), [ZnCl(PyAm)<sub>2</sub>]<sub>2</sub>[ZnCl<sub>4</sub>]·C<sub>2</sub>H<sub>5</sub>OH (4, monoclinic, P2<sub>1</sub>/n), and [ZnCl(PyAm)<sub>2</sub>]<sub>2</sub>Cl·CH<sub>3</sub>OH (5, triclinic, P-1). They comprised the same [ZnCl(PyAm)<sub>2</sub>]<sup>+</sup> monocation with a butterfly-like shape provided by the bidentate chelate coordination of two PyAm neutral entities and a chloride ligand. In a similar butterfly shape, ionic complex  $[ZnCl(PmAm)_2]_2[ZnCl_4]$  (6, monoclinic, C2/c) comprised the mononuclear [ZnCl(PmAm)<sub>2</sub>]<sup>+</sup> cations with two bidentate chelate-coordinated 2-amidinopyrimidine (PmAm) as neutral ligands. The Zn(II) pentacoordinated arrangement in 3-6 was variable, from square pyramidal to trigonal bipyramidal. The reported compounds' synthetic protocols, crystal structures and photoluminescence properties are discussed.

**Keywords:** zinc; multidentate ligands; X-ray crystallography; photoluminescence; coordination compounds; pseudopolymorphs



Citation: Nijhuis, M.R.; Yamba, Z.; Novikov, E.; Fonari, M.S.; Timofeeva, T.V.; Castañeda, R. A Series of Zinc Mononuclear Complexes with Imidoyl Amidine Ligands: Syntheses, Crystal Structures, and Photoluminescence Properties. Chemistry 2024, 6, 760–772. https:// doi.org/10.3390/chemistry6040045

Academic Editor: Narcis Avarvari

Received: 20 June 2024 Revised: 15 August 2024 Accepted: 16 August 2024 Published: 20 August 2024



Copyright: © 2024 by the authors. Licensee MDPI, Basel, Switzerland. This article is an open access article distributed under the terms and conditions of the Creative Commons Attribution (CC BY) license (https://creativecommons.org/licenses/by/4.0/).

# 1. Introduction

Zinc, the 23rd most abundant element in the earth's crust, is essential for human being and modern living and stands fourth among all metals in world production, thus being exceeded only by iron, aluminum, and copper. The importance of Zn(II) coordination complexes becomes apparent from many applications, like in therapeutic roles against biologically relevant peptide/protein targets [1], anticancer agents [2], in chemo/biosensors [1,3,4], magnetic resonance imaging (MRI) contrast agents [5,6], as catalysts in organic chemistry [7], and low-cost organic light-emitting devices (OLEDs) [8]. All the aforementioned applications make use of many Zn advantages, particularly highlighting its low toxicity and photoluminescence (PL) properties. Specifically, complexes based on Zn(II) cation are widely utilized due to their luminescent properties, enhancing the versatility of luminescent levels in both solution and the solid state. Notably, various Zn(II) complexes played crucial role in these breakthroughs when the powerful luminophores were attached to the d<sup>10</sup> close-shell Zn(II) atom [9–14].

Amidine chromophores, due to their multidentate scaffold and possibility to take different tautomeric forms, have been documented as good complexing agents [15]. In contrast

to amidine chemistry, only a few reports exist for the synthesis of aryl *N*-imidoylamidines [16], and until recently, ligand framework *N*-2-pyridylimidoyl-2-pyridylamidine (Py<sub>2</sub>ImAm) was generated only through one-pot metal-assisted transformations [17]. Brusso's group [18,19] reported the reliable synthesis of Py<sub>2</sub>ImAm on a large scale without the necessity for metal ion assistance [18] and explored its selective coordination in a bidentate and/or tridentate fashion [19]. Ever since the synthesis and isolation of Py<sub>2</sub>ImAm and Pm<sub>2</sub>ImAm (*N*-2-pyrimidylimidoyl-2-pyrimidylamidine) were reported, mono- di-, tri-, and tetranuclear complexes with various first-row transition metals, like manganese [19,20], iron [19,20], cobalt [19,21], copper [22], and nickel [22], have been documented by Castañeda et al. The same group of authors succeeded in the synthesis of lanthanide complexes with 2-amidinopyridine (PyAm) and 2-amidinopyrimidine (PmAm) as the products of metal-assisted hydrolysis of Py<sub>2</sub>ImAm and Pm<sub>2</sub>ImAm. The Eu(III), Tb(III), and Dy(III) complexes exhibited characteristic emissions of red, green, and yellow light reinforced by the coordinated PyAm and PmAm ligands as suitable sensitizers [23,24].

The lack of structural information on Zn(II) complexes with Py<sub>2</sub>ImAm, PyAm, and PmAm ligands (Scheme 1), and the reported examples of the blue emitted Zn(II) complexes with N-donor bases [12–14], sparked our interest in this research. The synthetic protocols, crystal structures, and photoluminescence properties of a series of Zn(II) complexes with these three ligands, which are novel and promising in their applications, are presented here.

**Scheme 1.** Structural formulas of the ligands used for synthesis of Zn complexes.

# 2. Materials and Methods

### 2.1. General

All solvents and reagents were of reagent grade and used without further purification, unless stated otherwise. Zinc(II) chloride (ZnCl<sub>2</sub>) was purchased from Ward's Science and used as Lab Grade. Triethylamine (TEA) was purchased from Alfa Aesar with a purity of 99%. *N*-2-pyridylimidoyl-2-pyridylamidine (Py<sub>2</sub>ImAm) was synthesized according to a procedure from the literature [18]. 2-Amidinopyridine (PyAm) was purchased from AmBeed. 2-Amidinopyrimidine was synthesized according to the reported procedure [25].

FT-IR spectra were collected on a Perkin Elmer–Spectrum Two FT-IR Spectrophotometer (4000–450 cm $^{-1}$ ) loaded with Perkin Elmer UATR Two, featuring a diamond prism center for solid-state IR measurements. Raman spectra were recorded on a Thermo-scientific DXR3 Smart Raman instrument fitted with a 180-degree accessory, a DXR 785 nm HP laser, and Omnic spectroscopy software (Thermo-scientific, Waltham, MA, USA). Solid-state emission spectra were recorded on a Shimadzu RF-5301PC spectrofluorophotometer loaded with a Xe lamp and RFPC software Rev. B.01.01 at  $\lambda_{\rm exc}=250$  nm for 1 and 3, and  $\lambda_{\rm exc}$  330 nm for 2 and 6. Microscopic images of crystals were obtained using the 4X Plan N lens on the Olympus BX51TRF Digital Microscope, which uses ImageView (version X64, 3.7) software (Figure S1).  $^{1}$ H NMR was collected on a Bruker Advance III 300 MHz NMR.

### 2.2. Synthesis

### 2.2.1. Synthesis of $[Zn(Py_2ImAm)_2]$ (1)

The metal salt  $ZnCl_2$  (0.0386 g, 0.283 mmol) was dissolved in 4 mL of methanol in a glass tube. In a separate tube the ligand  $Py_2ImAm$  (0.1979 g, 0.880 mmol) was dissolved in 21.6 mL of acetonitrile (MeCN) and 2.4 mL of TEA. Then, the  $ZnCl_2$  solution was slowly

and carefully layered on top of the  $Py_2ImAm$  solution. After that, the tube was sealed with a stopper and left for six days. Compound  $[Zn(Py_2ImAm)_2]$  crystallized as colorless block-like crystals. After crystallization, the crystals were filtered off using gravitational filtration. Yield 0.1003 g (0.195 mmol, 68.9%). IR (cm<sup>-1</sup>):  $\nu$  3314 (w), 3298 (w), 3261 (m), 1574 (w), 1544 (m), 1476 (s), 1447 (s), 1424 (s), 1290 (w), 1265 (m), 1229 (m), 1154 (w), 1051 (m), 996 (m), 875 (w), 851 (w), 815 (m), 748 (s), 701 (s), 649 (m), 623 (m), 568 (m). Raman (cm<sup>-1</sup>): 1599 (s), 1548 (m), 1480 (s), 1417 (w), 1205 (s), 1189 (m), 1101 (w), 1058 (m), 999 (s), 919 (w), 627 (w), 278 (w), 197 (s).

## 2.2.2. Synthesis of [ZnCl<sub>2</sub>(Py<sub>2</sub>ImAm)] (2)

The metal salt ZnCl<sub>2</sub> (0.0667 g, 0.492 mmol) was dissolved in 4 mL of methanol in a glass tube. In a separate tube, the ligand Py<sub>2</sub>ImAm (0.1738 g, 0.772 mmol) was dissolved in 10.8 mL of MeCN. Then, the ZnCl<sub>2</sub> solution was slowly and carefully layered on top of the Py<sub>2</sub>ImAm solution. Crystal formation was seen upon layering. Compound [ZnCl<sub>2</sub>(Py<sub>2</sub>ImAm)] was crystallized as colorless rod-shaped crystals. After crystallization completed, the crystals were filtered out using gravitational filtration. Yield: 0.0641 g (0.486 mmol, 36.2%). IR (cm<sup>-1</sup>):  $\nu$  3269 (m), 3077 (w), 3058 (w), 1635 (s), 1594 (s), 1584 (s), 1567 (s), 1496 (m), 1467 (m), 1436 (s), 1361 (s), 1295 (m), 1261 (m), 1200 (m), 1184 (s), 1141 (m), 1048 (w), 1024 (m), 1015 (s), 1006 (s), 900 (s), 781 (s), 753 (s), 703 (w), 662 (w), 638 (s), 596 (s). Raman (cm<sup>-1</sup>): 1590 (s), 1500 (s), 1360 (w), 1206 (w), 1144 (m), 1048 (m), 1017 (m), 791 (w), 702 (w), 640 (w), 489 (w).

# 2.2.3. Synthesis of [ZnCl(PyAm)<sub>2</sub>]Cl (3) and ZnCl(PyAm)<sub>2</sub>]<sub>2</sub>[ZnCl<sub>4</sub>]·C<sub>2</sub>H<sub>5</sub>OH (4)

In separate vials, 2-aminopyridine hydrochloride (73 mg; 0.46 mmol) and ZnCl<sub>2</sub> (136.6 mg; 1 mmol) were dissolved using 4 mL and 2 mL of ethanol, respectively, under atmospheric conditions. To the ligand's solution, 0.3 mL of triethylamine was added. After that, both solutions were combined, and the flask was sealed with parafilm. Overnight, a small quantity of crystals, which we called crystals 4, grew at the vial's walls. These crystals were separated from the walls and placed in a separate container. After five days, colorless crystals of 3 were formed as precipitate, filtered off from the mother liquor, and rinsed with ethanol. So, both crystals 3 and 4 were recovered from the same vial, but after different numbers of days. Under the microscope, both crystals looked similar; however, the crystals of 4 were larger. Yield of 3 53.3 mg (0.41 mmol, 90%). IR of 3  $\nu$  (cm<sup>-1</sup>): 3378 (w), 3315.5 (m), 3277 (w), 3218 (s), 3164 (w), 3061 (w), 1652 (s), 1605 (w), 1583 (w), 1563 (s), 1511 (m), 1463 (s), 1443 (w), 1436 (m), 1309 (w), 1276 (w), 1254 (m), 1175 (w), 1158 (w), 115 (w), 1085 (w), 1051 (w), 1010 (s), 975 (w), 963 (w), 909 (w), 864 (s), 813 (s), 802 (m), 759 (m), 741 (s), 684 (w), 670 (w), 635 (m). X-ray analysis allowed for us to deduce that crystals 3 and 4 represent different crystalline forms whose nature is described below.

# 2.2.4. Synthesis of [ZnCl(PyAm)<sub>2</sub>]<sub>2</sub>Cl·CH<sub>3</sub>OH (5)

The reaction was conducted under atmospheric conditions. In different tubes, 2-amidinopyridine hydrochloride (31.8 mg; 0.2 mmol) and  $\rm ZnCl_2$  (25 mg; 0.18 mmol) were dissolved using 3 mL and 2 mL of methanol, respectively. To the ligand's solution, 0.2 mL of triethylamine was added. Afterwards both solutions were combined; the tube was sealed with parafilm and left to slowly evaporate. Only few colorless crystals were formed at the walls of the tube. If the reaction was left for complete solvent evaporation, no crystals were obtained, likely due to methanol loss from the crystal lattice and the crystal deterioration.

### 2.2.5. Synthesis of $[ZnCl(PmAm)_2]_2[ZnCl_4]$ (6)

The ligand PmAm (0.833 mmol, 100.30 mg) was dissolved in 4 mL of chloroform. In a separate vial,  $ZnCl_2$  (0.641 mmol, 87.60 mg) was dissolved in 2 mL of ethanol. Afterwards, the  $ZnCl_2$  solution was filtered on the top of the ligand's solution. The ligand-to- $ZnCl_2$  molar ratio was 2:1. The resultant solution was placed in a vial, sealed with parafilm, and allowed to crystallize for 5 days. Colorless crystals formed, which were filtered out, rinsed

with chloroform, and weighed. After filtration, the yield of the product was 10%. IR v (cm $^{-1}$ ): 3331 (m), 2981 (w), 1655 (s), 1585 (s), 1498 (m), 1402 (s), 1243 (w), 1193 (w), 1065 (w), 1011 (w0, 831 (s), 806 (w), 746 (m), 669 (m), 641 (m), 571 (m).  $^{1}$ H-NMR (300 MHz, D<sub>2</sub>O)  $\delta$ : 8.85 (d, 2H), 7.68 (t, 1H).

### 2.3. X-ray Single-Crystal Structure Determination

Crystals 1–6, suitable for single-crystal X-ray diffraction (SCXRD) analysis were covered in parabar oil and mounted on a cactus needle. The diffraction data for all samples were collected at 100 K on a Bruker Smart Apex-II CCD Diffractometer with MoK  $\alpha$  ( $\lambda$  = 0.71073). The diffraction measurement method was  $\varphi$  and  $\omega$  scans. The multi-scan absorption correction was performed using SADABS-2016/2 (Bruker, 2016/2) [26]. The structures were solved with the ShelXT structure solution program package and refined by full-matrix least squares on  $F^2$  by use of all reflections with the ShelXL refinement package [27]. Non-hydrogen atoms were refined with anisotropic displacement parameters. C-bound hydrogen atoms were included in calculated positions (riding model), while N-bound imino- and amino-hydrogen atoms were located in difference Fourier maps and refined in isotropic approximation by applying soft distance restraints [28]. Crystal data for 1–6 are summarized in Table 1, selected bond distances and angles are listed in Table S1, and hydrogen bond parameters are listed in Table S2. CCDC deposition numbers are 2357006–2357011.

Table 1. Crystal data and structure refinement parameters for 1–6.

Compound	1	2	3	4	5	6
Empirical formula	$C_{24}H_{20}N_{10}Zn$	$C_{12}H_{11}Cl_2N_5Zn$	$C_{12}H_{14}Cl_2N_6Zn$	C <sub>26</sub> H <sub>34</sub> Cl <sub>6</sub> N <sub>12</sub> OZn <sub>3</sub>	C <sub>13</sub> H <sub>18</sub> Cl <sub>2</sub> N <sub>6</sub> OZn	C <sub>20</sub> H <sub>24</sub> Cl <sub>6</sub> N <sub>16</sub> Zn <sub>3</sub>
<i>FW</i> (g mol <sup>-1</sup> )	513.87	361.53	378.56	939.46	410.60	897.36
Temperature, K	100(2)	100(2)	100(2)	100(2)	100(2)	100(2)
Crystal system	monoclinic	monoclinic	triclinic	monoclinic	triclinic	monoclinic
Space group	$P2_1/c$	$P2_1/n$	P-1	$P2_1/n$	P-1	C2/c
a/Å	10.6286(19)	8.7118(4)	7.8719(15)	9.8693(8)	7.0080(6)	13.4968(10)
b/Å	23.985(5)	14.6347(5)	8.5598(16)	14.1886(12)	9.6020(7)	13.1249(11)
c/Å	9.4821(16)	10.6399(4)	12.994(3)	26.130(2)	13.1569(10)	19.6259(17)
α/deg	90	90	96.765(3)	90	91.723(6)	90
β/deg	101.948(6)	95.961(4)	103.846(3)	92.433(4)	96.864(5)	108.024(2)
$\gamma/{ m deg}$	90	90	110.895(3)	90	101.139(5)	90
$V/\text{Å}^3$	2364.8(7)	1349.19(9)	774.0(3)	3655.7(5)	861.15(12)	3306.0(5)
Z	4	4	2	4	2	4
D <sub>calcd</sub> g/cm <sup>3</sup>	1.443	1.780	1.624	1.707	1.584	1.803
$\mu/\text{mm}^{-1}$	1.073	2.211	1.933	2.433	1.748	2.687
Reflections collected	28857	12768	19834	42016	26373	28609
Independent reflections	4642 [R(int) = 0.0362]	3940 [R(int) = 0.0369]	4312 [R(int) = 0.0313]	7421 [ <i>R</i> (int) = 0.0449]	4922 [R(int) = 0.0334]	4815 [R(int) = 0.0269]
GOF	1.036	1.032	1.045	1.023	1.042	1.072
$R_1$ , $wR_2$ $(I > 2\sigma(I))$	0.0304, 0.0713	0.0428, 0.1101	0.0258, 0.0624	0.0298, 0.0626	0.0262, 0.0623	0.0257, 0.0665
$R_1$ , $wR_2$ (all data)	0.0441, 0.0766	0.0633, 0.1260	0.0331, 0.0655	0.0446, 0.0673	0.0336, 0.0652	0.0332, 0.0688
Largest diff. peak and hole/e·Å <sup>-3</sup>	0.245 and -0.282	1.550 and -1.012	0.435 and -0.294	0.818 and -0.457	0.431 and -0.405	0.723 and -0.312

#### 3. Results

In the synthetic procedures, similar approaches were used. The amidine ligand was first dissolved in an organic solvent, such as acetonitrile or chloroform, and an alcoholic solution (methanol or ethanol) of a metal salt was layered on top of the ligand's solution. The reaction solution was typically left for a day and the crystals were formed in different ways, including but not limited to right upon layering, at the layer, or growing on the walls of the reaction tube. Complexes 4 and 5 contain ethanol or methanol in the crystal lattice, and as a result, they experience solvent loss over time. Complexes 3 and 4 grow in the same vial.

### 3.1. Crystal Structures of Complexes

Coordinating the tridentate or bidentate sites of  $Py_2ImAm$  ligand can be achieved by using an acid or a base, respectively [19]. Following that route, Zn(II) was coordinated to both individual sites in  $Py_2ImAm$  (Scheme 2). For the bidentate ligand coordination complex  $[Zn(Py_2ImAm)_2]$  (1), a methanolic solution of the metal salt  $ZnCl_2$  was layered on top of  $Py_2ImAm$  solution in MeCN and TEA, resulting in the desired compound. The attempts to use MeCN, DCM, DMSO, or CHCl<sub>3</sub> combined with either MeOH or EtOH to obtain this compound were unsuccessful. It is important to recall the same solvents are used to coordinate either the bidentate or tridentate sites, and the main difference in the synthesis was the presence or absence of a weak base such as TEA.

**Scheme 2.** The synthetic pathway to the complexes  $[Zn(Py_2ImAm)_2]$  (1) and  $[ZnCl_2(Py_2ImAm)]$  (2).

The mononuclear complex  $[Zn(Py_2ImAm)_2]$  (1) crystallizes in the monoclinic space group  $P2_1/c$  (Table 1). The asymmetric unit comprises one Zn(II) cation, and two  $Py_2ImAm$  ligands as monoanions that coordinate the metal in the bidentate chelate binding modes. Zn atoms take an  $N_4$ -tetrahedral coordination geometry with the Zn-N bond distances being in the range 1.9632(16)-1.9797(19) Å (Table S1), which is within the range commonly observed for N-Zn(II) bonds in the CSD database [29]. The Zn(II) distorted tetrahedral geometry is confirmed by the calculated geometry index value  $\tau_4 = 0.81$  [30]. Each of two virtually planar six-membered chelato-metallocycles are coplanar with the pyridine rings anchored to it, the planar conformation being additionally stabilized by intramolecular NH...N short contacts (Table S2). The complex as a whole has a two-blade-propeller shape with an interplanar angle of  $65.20(2)^\circ$  between the two almost planar  $Py_2ImAm$ 

platforms (Figure 1a). The closest structural analogues to 1 are Pd(II) [17], Co(II) [21], Ni(II) [31], and Cu(II) [32] and have square planar metal's coordination geometries. The cross-shape complexes of 1 are self-associated via NH...N hydrogen bonds (Table S2) into an H-bonded chain running along the crystallographic c axis (Figure 1b). In the crystal, stacking patterns were registered between the pyridines' rings with the separations Cg(N5, C8 > C12)...Cg(N5, C8 > C12)(2 - x, 1 - y, 1 - z), 4.1027(15) Å, slippage 1.899 Å, Cg(N10, C20 > C24)...Cg(N10, C20 > C24)(1 - x, 1 - y, -z) 3.9270(17) Å, slippage 1.621 Å (Figure 1c).

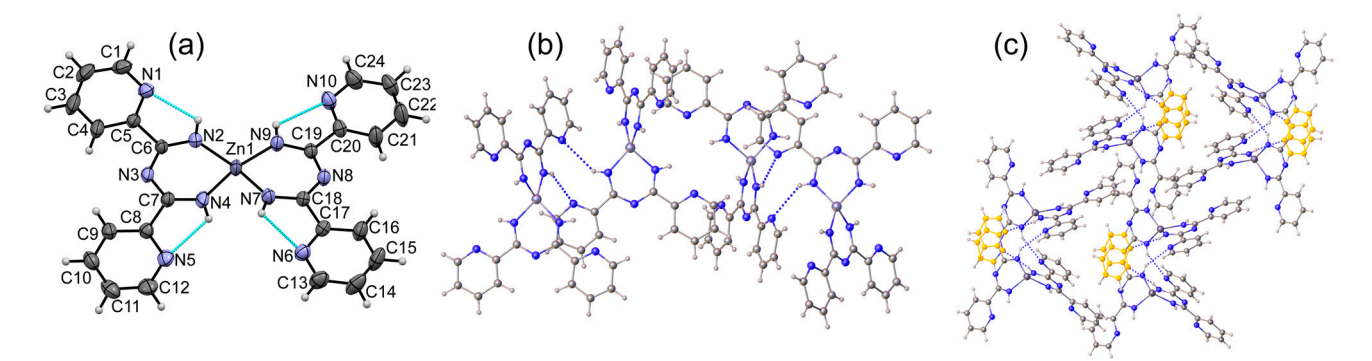


**Figure 1.** (a) View of complex **1**. Thermal ellipsoids are drawn with 50% probabilities; (b) H-bonded chain; (c) packing of H-bonded chains,  $\pi$ – $\pi$  stacking has been highlighted in yellow.

Notably, in the absence of a basic TEA component in the synthesis, the resulting interaction product between zinc chloride and Py<sub>2</sub>ImAm represented monoclinic crystals  $(P2_1/n \text{ space group, Table 1})$  with the composition  $[ZnCl_2(Py_2ImAm)]$  (2) where Zn(II)cation was coordinated to the tridentate pocket of Py<sub>2</sub>ImAm as a neutral ligand (Figure 2a). Within 2 Py<sub>2</sub>ImAm exists in the amino-imino tautomeric form (Scheme 1) confirmed by the reliable localization of the N-bound hydrogen atoms and distribution of C-N bond lengths in the ligand's scaffold (Figure 2a). The tridentate-chelate coordination of Py<sub>2</sub>ImAm occurs via two fused five-membered metallo-chelate rings. Completing the Zn(II) coordination core are two chloride ions, one approximately in the ligand plane and one above this plane. Due to the presence of a neutral ligand instead of anionic ligand, the Zn-N bond distances are longer than in complex 1 (2.074(2)-2.181(2) Å); Zn-Cl bond distances have the values 2.2917(7) and 2.2980(7) Å. For complex 2, a distorted square-pyramidal coordination geometry was confirmed by the  $\tau_5 = 0.17$  [33]. The planar skeleton of Py<sub>2</sub>ImAm is reinforced by intramolecular N(4)-H(4A)···N(2) hydrogen bond (Table S2). It is worth mentioning that 2 is isostructural with Mn(II) and Co(II) analogues with the same organic ligand and halide atoms [19]. In the crystal lattice, complexes are self-assembled via two NH...Cl hydrogen bonds in the double layers parallel to the  $(-1 \ 0 \ -1)$  plane with ligands situated in parallel planes separated by 3.341 Å (Figure 2b,c). The meaningful  $\pi$ – $\pi$  stacking interactions were registered with the involvement of pyridine (Py) and metallo-chelate rings as indicated by the centroid(Cg)...centroid(Cg) distances, Cg(Zn1, N1, C5, C6, N3)...Cg(Zn1, N1, C5, C6, N3(1 - x, 1 - y, 1 - z) 3.8433(13) Å, slippage 1.811 Å; Cg(Zn1, N1, C5, C6, N3)...Cg(N1, C1)> C5)(1 - x, 1 - y, 1 - z) 3.5990(14) Å, and Cg(N1, C1 > C5)...Cg(N5, C8 > C12)(1/2 - x, -1/2 + y, 1/2 - z) 3.5809(15) Å.

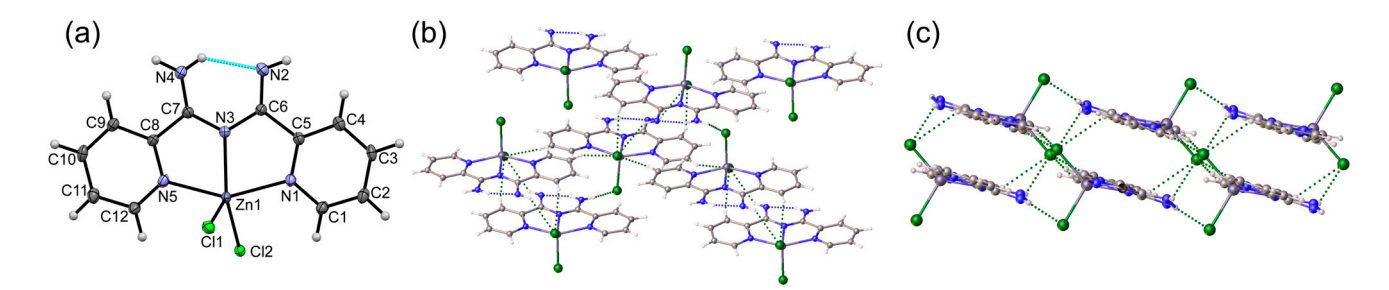


**Figure 2.** (a) View of complex **2**. Thermal ellipsoids are drawn with 50% probabilities; (b) top view of H-bonded double layer in **2**; (c) side view of H-bonded stacking double layer in **2**.

Complex [ZnCl(PyAm)<sub>2</sub>]Cl (3) crystallizes in the triclinic P-1 space group, and the asymmetric unit comprises one mononuclear cation [ZnCl(PyAm)<sub>2</sub>]<sup>+</sup> and one chloride counterion. Two neutral PyAm ligands coordinate Zn(II) (Figure 3a) with an imino nitrogen (N2 and N5) and a pyridine nitrogen (N1 nad N4; Figure 3a). Zn(II) atom takes a square-pyramidal coordination geometry with four nitrogen atoms in the basal plane (rms deviation of these N-atoms is 0.0537 Å; the Zn atom deviation from this plane is 0.6375(7) Å). The distorted square-pyramidal Zn(II) coordination geometry is confirmed by the  $\tau_5 = 0.17$  [34]. The Zn-N bond distances are in the range of 1.9954(13)–2.2790(13) Å, and the Zn-Cl distance is 2.2732(6) Å (Table S1). The mononuclear cation [ZnCl(PyAm)<sub>2</sub>]<sup>+</sup> has an inverse umbrella shape with the interplanar angle between two PyAm residues of 41.33(6)°. The crystal packing is reinforced by NH...Cl hydrogen bonds with participation of all NH-donors, and chloride anions as single (the coordinated Cl(1)) and multiple (outersphere Cl(2) chloride anion) H-acceptors (Table S2). Through the N(6)H...Cl(1) H-bond, the complex cations are linked in the translational chain running along the crystallographic a axis; through the outer-sphere Cl2<sup>-</sup> chloride anions, these chains are linked into the H-bonded layer; all H-bonds of NH...Cl type are realized within this layer (Figure 3b,c). The  $\pi$ ... $\pi$  stacking interactions between PyAm residues were found inside and between the layers, stacked along the crystallographic *c* axis (Figure 3c); meaningful contributions are Cg(N1, C1 > C5)...Cg(N1, C1 > C5)(1 - x, 1 - y, 1 - z) 3.5888(13) Å, slippage 1.003Å; and Cg(N4, C7 > C11)...Cg(N4, C7 > C11)(1 - x, -y, -z) 3.5888(12) Å, slippage 1.235 Å.

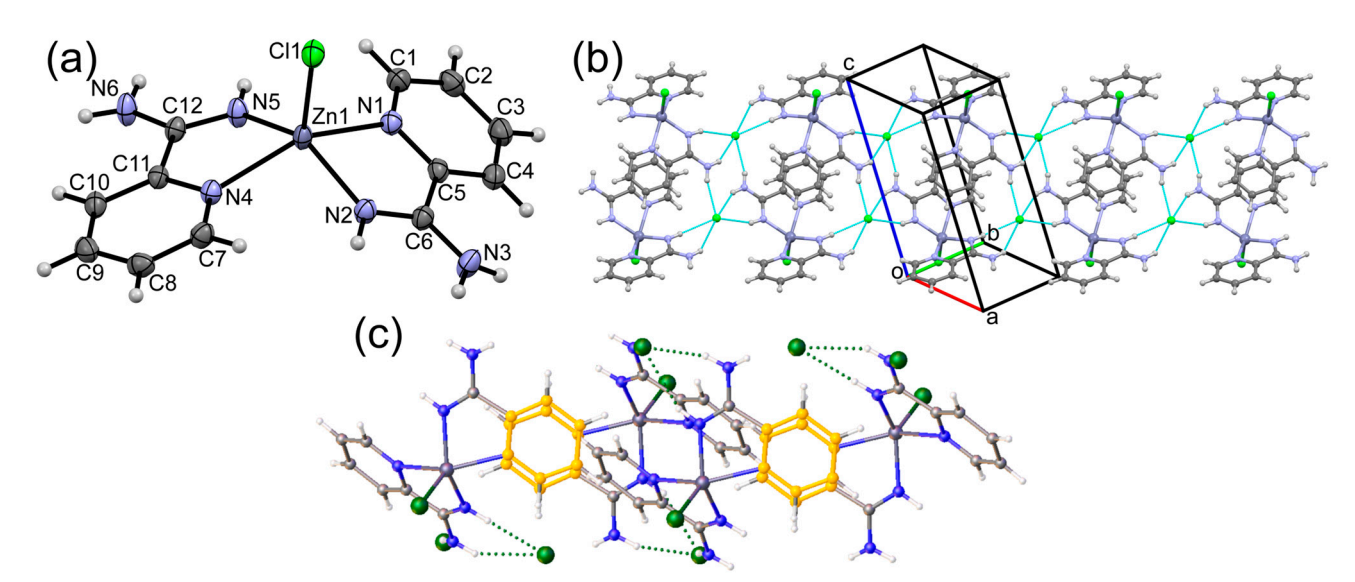


**Figure 3.** (a) View of complex **3**. Thermal ellipsoids are shown with 50% probabilities; (b) fragment of H-bonded double layer; (c) packing of H-bonded layers,  $\pi$ – $\pi$  stacking has been highlighted in yellow.

Compound  $[ZnCl(PyAm)_2]_2[ZnCl_4]\cdot C_2H_5OH$  (4) crystallizes in the monoclinic  $P2_1/n$  space group (Table 1), and the asymmetric unit comprises two crystallographically unique

[ZnCl(PyAm)<sub>2</sub>]<sup>+</sup> monocations, one charge-balanced [ZnCl<sub>4</sub>]<sup>2-</sup> anion, and one EtOH solvent molecule; all species reside in general positions (Figure 4a). The distribution of Zn-N and Zn-Cl bond distances in [ZnCl(PyAm)<sub>2</sub>]<sup>+</sup> cations is quite similar between two of them, and close to 3 (Table S1). However, the more accurate examination of Zn(II) coordination geometries revealed distinctions in the Zn(1) and Zn(2) coordination cores (Figure 4b). Namely, the atom Zn(2) adopts a square-pyramidal coordination geometry with four nitrogen atoms situated in the basal plane with the rms deviation of these N-atoms being 0.0695 Å, and the Zn(2) atom deviation from this plane being 0.481(1) Å. The square-pyramidal Zn(2) coordination geometry is also confirmed by  $\tau_5 = 0.17$  [33]. Otherwise, for Zn(1), the wider scattering in the N<sub>4</sub> deviations from the mean plane (rms deviation of four N-atoms is 0.3829 Å) and in bond angles (Table S1) was observed. The coordination geometry of Zn(1) corresponds to the trigonal bipyramidal with the pyridyl N atoms occupying the axial positions. The calculated  $\tau_5$ -index of 0.78 also indicates the distorted trigonal bipyramidal coordination geometry for Zn(1) atom. The NH...Cl hydrogen bonds are driving forces in 4 that assemble the charged species. The complex cations [Zn(1)Cl(PyAm)<sub>2</sub>]<sup>+</sup> are associated in the H-bonded chain through tetrahedral [ZnCl<sub>4</sub>]<sup>2-</sup> counterions and EtOH solvent molecules (Figure 4c) with the meaningful stacking patterns with involvement of both pyridine rings, as indicated by the distances  $Cg(N9, C15 > C19) \dots Cg(N9, C15 > C19)(1 - x, -y,$ 1-z) 3.8847(16) Å, slippage 1.875 Å, and Cg(N12, C21 > C26)...Cg(N112, C21 > C26)(1 - x, 1 - y, 1 - z) 3.9557(15) Å, slippage 1.803 Å (Figure 4c). Cations  $[Zn(2)Cl(PyAm)_2]^+$  are self-assembled in dimers that are H-bonded with the [ZnCl<sub>4</sub>]<sup>2-</sup> counterions (Figure 4d).

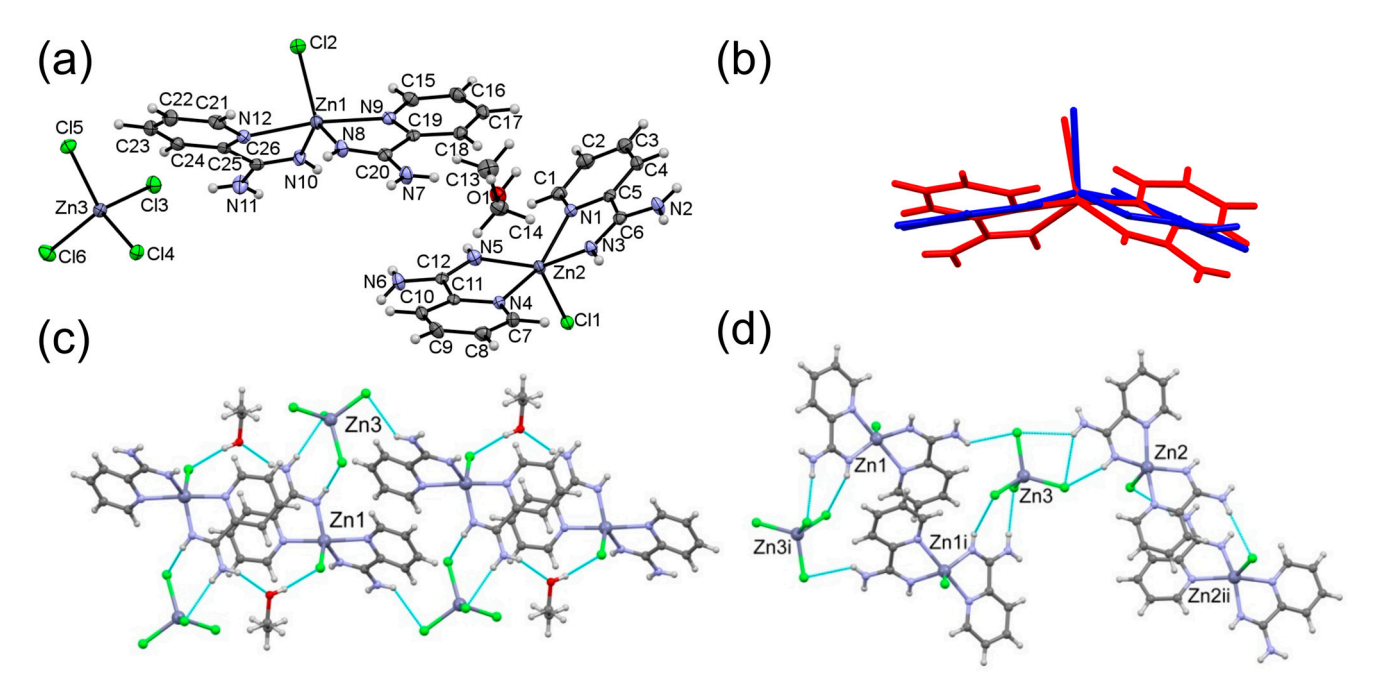


**Figure 4.** (a) Content of the asymmetric unit in **4**. Thermal ellipsoids are shown with 50% probabilities. (b) The overlay diagram for two  $[Zn(PyAm)_2Cl]^+$  cations; (c) fragment of H-bonded chain with involvement of Zn(1) cation; (d) fragment of crystal packing showing different H-bonded association patterns with an indication of the symmetry-related atoms. (i) 1 - x, -y, 1 - z; (ii) 3/2 - x, 1/2 + y, 1/2 - z.

Despite the intrusion of solvent methanol molecules, compound [ZnCl(PyAm)<sub>2</sub>]<sub>2</sub>Cl·CH<sub>3</sub>OH (5) reproduces the principal structural features of compound 3. Similar to 3, complex 5 crystallizes in the triclinic P-1 space group (Table 1), and the asymmetric unit comprises one mononuclear cation [ZnCl(PyAm)<sub>2</sub>]<sup>+</sup>, charge-balanced chloride anion and methanol solvent molecule (Figure 5a). The structure of cation in 5 differs insignificantly from that in 3, the Zn-N bond distances vary in the range 2.0034(12)–2.2089(12) Å, and Zn-Cl bond distance is equal to 2.2895(4) Å (Table S1). The interplanar angle between two bidentate chelate PyAm

residues is slightly larger, at  $51.49(3)^{\circ}$ . The Zn(II) coordination geometry in between trigonal bipyramidal and square pyramidal, as indicated by the calculated value  $\tau_5 = 0.58$  [33]. In a similar way as in 3, the crystal packing in 4 is reinforced by NH...Cl hydrogen bonds with participation of all NH-donors, and both coordinated Cl-ligand and outer-sphere Cl<sup>-</sup> anion as multiple H-acceptors (Table S2). The methanol solvent molecules mediate chloride anions and complex cations as single H-donors through OH...Cl<sup>-</sup> hydrogen bonds, and as single H-acceptors through NH...O hydrogen bonds. These H-bonds combine the species in H-bonded layers (Figure 5b) parallel to the (1 0 0) crystallographic plane, and the layers stack along the crystallographic a axis with the methanol molecules situated in the interlayer space (Figure 5c). The  $\pi$ ... $\pi$  stacking interactions between PyAm residues were found inside and between the layers, the most meaningful impacts provide interactions between metallo-chelate rings, Cg(Zn1, N4, N5, C7, C8)...Cg(Zn1, N4, N5, C7, C8) 4.2903(8) Å, slippage 2.615 Å; and between the pyridine's rings, Cg(N3, C2 > C6)...Cg(N3, C2 > C6)(1 - x, -y, -z) 3.4458(9) Å, slippage 1.539 Å.

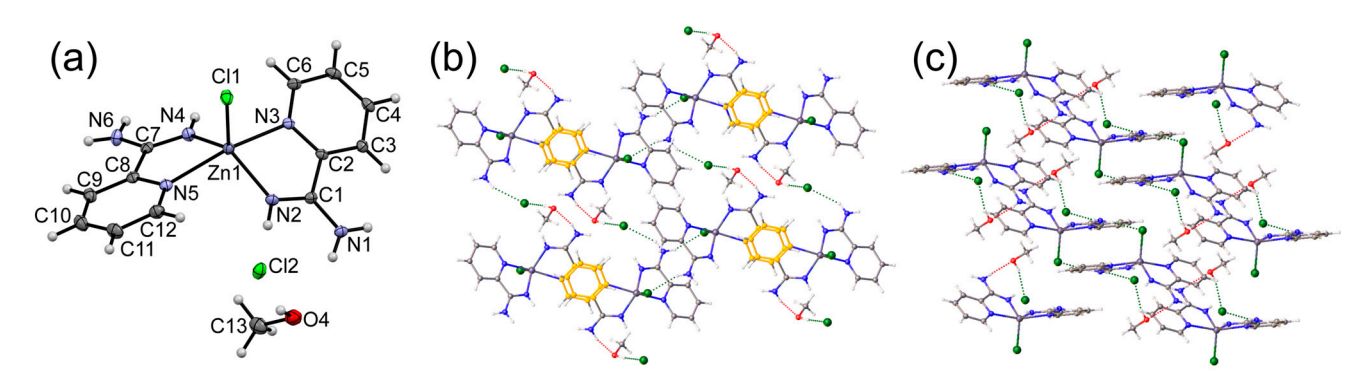


**Figure 5.** (a) View of complex **5**. Thermal ellipsoids are shown with 50% probability; (b) fragment of H-bonded double layer,  $\pi$ – $\pi$  stacking has been highlighted in yellow; (c) packing of H-bonded layers.

A close structural analogue for 3–5 was found in the CSD database with PyAm ligand in its neutral form [34]. This analogous structure is a mononuclear coordination complex  $[ZnCl(PyAm)_2]Cl\cdot 2H_2O$ , where the ligand PyAm was prepared in situ through the reaction of 2-cyanopyridine with LiN(SiMe<sub>3</sub>)<sub>2</sub> in the presence of  $ZnCl_2$  [34]. This structure has a butterfly-like shape similar to 3–5. All these complexes have in a common a short N-Zn distance (~1.99 Å) when the donor is the nitrogen atom in the imino group, and a longer N-Zn distance (~2.21 Å) when the coordinated nitrogen atom comes from the pyridine ring.

Compound  $[ZnCl(PmAm)_2]_2[ZnCl_4]$  (6) crystallizes in the monoclinic C2/c space group, and the asymmetric unit comprises one mononuclear cation, [ZnCl(PmAm)<sub>2</sub>]<sup>+</sup> and a half of charge-balanced [ZnCl<sub>4</sub>]<sup>2-</sup> counterion that obeys the two-fold symmetry (Figure 6a). Similar to 3–5, herein in mononuclear cation [ZnCl(PmAm)<sub>2</sub>]<sup>+</sup>, two neutral PmAm ligands coordinate the metal in the bidentate chelate binding modes, Zn-N distances being in the range 2.0103(14)–2.2280(14) Å, the shortest ones being the imino N4 and N5 atoms as the better electron donors (Table S1). Both PmAm ligands have virtually planar skeletons additionally fixed by intramolecular NH...N hydrogen bonds (Table S2), the interplanar angle between two PmAm residues being of 59.04(5)°. The pentacoordinate coordination geometry of Zn1 is completed by chloride ligand, Zn1-Cl1 distance being 2.2803(5) Å. The Zn(II) atom takes a trigonal-bipyramidal coordination, with the pyridyl N atoms occupying the axial positions. The calculated  $\tau_5 = 0.75$  [33] also indicated in favor of trigonal bipyramidal Zn(II) coordination geometry. The crystal packing is guided by NH...Cl hydrogen bonds with involvement of the tetrahedral  $[ZnCl_4]^{2-}$  anion. Each anion arranges around four complex cations forming the chiral H-bonded layer (Figure 6b). The layers pack in an antiparallel mode with the lack of strong interlayer interactions (Figure 6c). The only one meaningful  $\pi$ – $\pi$  stacking interaction in this structure is between

the inversion-related five-membered metallo-chelate rings, Zn1N3C2C1N4, with Cg. . . Cg separation of 4.2722(9) Å, and slippage of 2.809 Å.

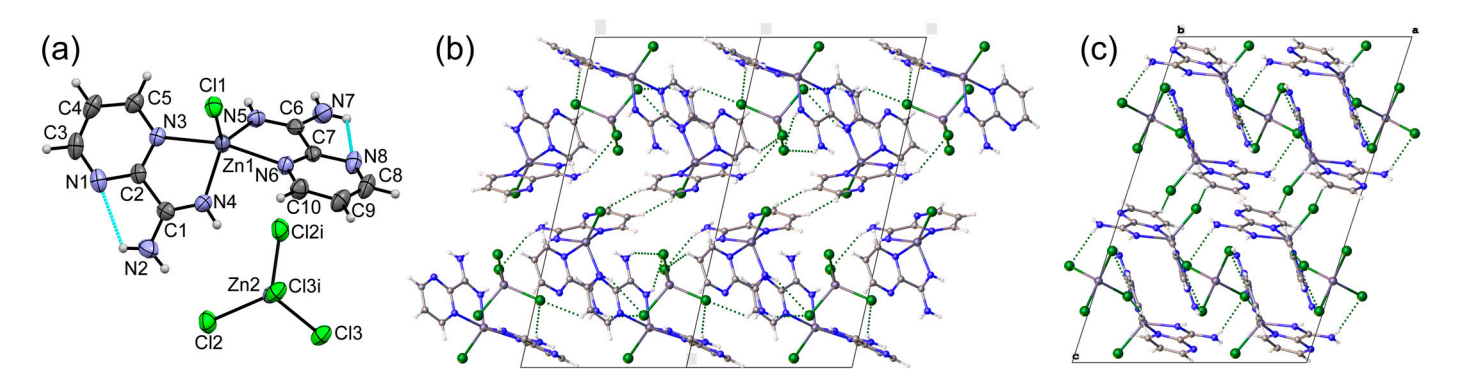


**Figure 6.** (a) Content of the asymmetric unit in **6**. Symmetry-related positions are labeled with 'i' 1 - x, y, 3/2 - z. (b) View of H-bonded layer; (c) packing of the two layers.

# 3.2. Photoluminescence Properties

The search for blue luminous materials for applications in blue light-emitting devices (LEDs) remains an ongoing interest in materials science [8–14]. Stable blue luminescent compounds that are useful in electroluminescent devices are still rare and very challenging to manufacture. In this paper, we are using a series of ligands to find out their effect on PL. Previous research of a series of zinc(II) complexes containing di-2-pyridylamine and 2,6-bis(2-pyridylamino) pyridine ligands were reported to exhibit blue PL emitted mostly at  $\lambda_{\text{max}}$  < 400 nm in solution and in the solid state [9]. However, compounds based on pyridylamines lack stability electroluminescent devices. The instability in these compounds was mostly due to the fact that the ligands in the complexes were negatively charged and hence susceptible to humidity. The efforts were therefore focused on stabilizing the charge on the negatively charged ligands and using neutral ligands [14]. With exception of 1, the complexes we are studying utilize neutral ligands that lack any emission. An interesting example of using similar ligands in previous results demonstrated the viability of PyAm as an antenna for the sensitization of lanthanide ions, typically achieved via chelating effects, thus stabilizing the Ln(III) coordination environment and providing an efficient energy transfer to the Ln(III) ions [23]. Taking all the above into account, the PL properties were studied for 1–3 and 6 in the solid state. The crystals were irradiated under short-wavelength UV light and revealed bright emission in the narrow range, 365–378 nm (Figure 7). Complexes 1 and 2, with the same ligand in either anionic or neutral form, exhibited similar emission spectra, with  $\lambda_{max} = 370$  nm for 1 and  $\lambda_{max} = 365$  nm for 2. When Zn was coordinated in the tridentate site of a Py<sub>2</sub>ImAm in 2, the emission was sharper and more blue-shifted, with  $\lambda_{max}$  of 365 nm. Complex 3 was unstable under light irradiation and decomposed shortly after data collection. The decomposition was observed as the emission decayed over time, and the initial complex changed color from white to blue. This is the likely explanation emission of this complex. The rest of the complexes were stable upon light excitation, without emission decay or changes from the original sample. Interestingly, out of all complexes, the emission maximum for 6 was mostly red-shifted with a  $\lambda_{em}$  = 378 nm. Both 1 and 6 have a minor emission peak that can be seen as a shoulder to the main peak. The positions of the emission maxima in the violet region of spectrum in 1-3 and 6 indicated in favor of the intraligand energy transfer due to the formation of the chelate metallocycle as the source  $\pi$ – $\pi$ \* intraligand excited state [14].

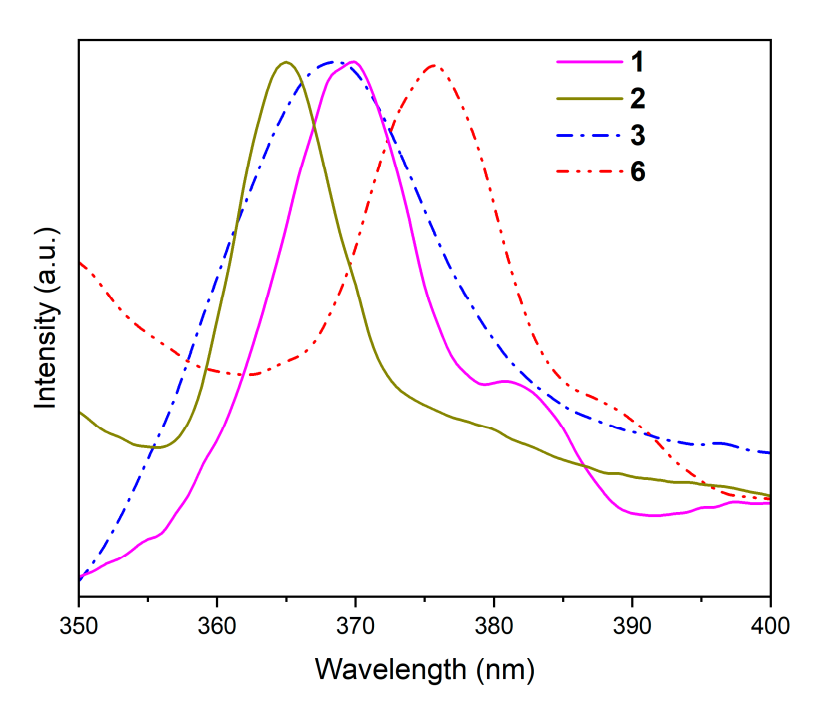


Figure 7. Normalized emission spectra of 1–3, 6 in the solid state.

### 4. Conclusions

Six new mononuclear complexes were obtained through the interaction of amidinebased ligands with zinc chloride. In the case of N-2-pyridylimidoyl-2-pyridylamidine (Py<sub>2</sub>ImAm), the metal ion was coordinated either with the bidentate pocket of the anionic imino-imino tautomeric form of the ligand in [Zn(Py<sub>2</sub>ImAm)<sub>2</sub>] (1) or with the tridentate pocket of neutral ligand in its imino-amino tautomeric form in [ZnCl<sub>2</sub>(Py<sub>2</sub>ImAm)] (2). The ionic crystals [ZnCl(PyAm)<sub>2</sub>]Cl (3), [ZnCl(PyAm)<sub>2</sub>]<sub>2</sub>[ZnCl<sub>4</sub>]·C<sub>2</sub>H<sub>5</sub>OH (4), [ZnCl(PyAm)<sub>2</sub>]<sub>2</sub> Cl·CH<sub>3</sub>OH (5), and [ZnCl(PmAm)<sub>2</sub>]<sub>2</sub>[ZnCl<sub>4</sub>] (6) (PyAm—2-amidinopyridine, PmAm—2amidinopyrimidine) comprise the similar butterfly-shaped mononuclear cations provided by the bidentate chelate coordination of two neutral 2-amidino-ligands, and chloride anions interconnected by hydrogen bonds. The Zn(II) atom revealed the N<sub>4</sub> or N<sub>4</sub>Cl sets of coordinated donor atoms, with different coordination geometries, from tetrahedral in 1 to tetragonal pyramidal and trigonal bipyramidal in 2-6. The cooperative intermolecular hydrogen bonds governed the supramolecular aggregations as H-bonded chains in 1 and different two-dimensional arrays in **2**–**6**, while the  $\pi$ – $\pi$  stacking interactions were registered with participation of pyridine and metallo-chelate rings. The photophysically passive in the visible range free amidine ligands revealed significant emission in the ultraviolet region of spectrum being coordinated to Zn(II) in 1–3 and 6.

**Supplementary Materials:** The following supporting information can be downloaded at: https://www.mdpi.com/article/10.3390/chemistry6040045/s1, Figure with crystal images, Tables of Hydrogen Bonds. CCDC deposition numbers are 2357006–2357011.

**Author Contributions:** M.R.N., Z.Y. and R.C. synthesized all the metal complexes in this paper. The single crystal X-ray characterization was carried out by E.N. and R.C. The solid-state photoluminescence studies were conducted by M.R.N., Z.Y. and R.C. Crystallographic pictures from cif files were derived using mercury by M.S.F. All authors contributed during the writing process. All authors have read and agreed to the published version of the manuscript.

**Funding:** The authors thank the National Science Foundation, DMR for the support of PREM project #2122108, and DMR for the support of MRI project #2320830. M.S.F. thanks the subprogram 011202 from the Ministry of Education and Research of R. Moldova.

Data Availability Statement: Data are contained within the article and Supplementary Materials.

**Acknowledgments:** We thank New Mexico Highlands University for their technical support. We thank the American Crystallographic Association Summer School for help collecting data for two structures.

Conflicts of Interest: The authors declare no conflicts of interest.

#### References

- Drewry, J.A.; Gunning, P.T. Recent Advances in Biosensory and Medicinal Therapeutic Applications of Zinc(II) and Copper(II) Coordination Complexes. Coord. Chem. Rev. 2011, 255, 459–472. [CrossRef]
- 2. Pellei, M.; Del Bello, F.; Porchia, M.; Santini, C. Zinc Coordination Complexes as Anticancer Agents. *Coord. Chem. Rev.* **2021**, 445, 214088. [CrossRef]
- 3. Gusev, A.; Braga, E.; Shul'gin, V.; Lyssenko, K.; Eremenko, I.; Samsonova, L.; Degtyarenko, K.; Kopylova, T.; Linert, W. Luminescent Properties of Zn and Mg Complexes on N-(2-Carboxyphenyl)Salicylidenimine Basis. *Materials* **2017**, *10*, 897. [CrossRef] [PubMed]
- 4. Gusev, A.; Shul'gin, V.; Braga, E.; Zamnius, E.; Kryukova, M.; Linert, W. Luminescent Properties of Zn Complexes Based on Tetradentate N<sub>2</sub>O<sub>2</sub>-Donor Pyrazolone Schiff Bases. *Dye. Pigment.* **2020**, *183*, 108626. [CrossRef]
- 5. Major, J.L.; Parigi, G.; Luchinat, C.; Meade, T.J. The Synthesis and in Vitro Testing of a Zinc-Activated MRI Contrast Agent. *Proc. Natl. Acad. Sci. USA* **2007**, *104*, 13881. [CrossRef] [PubMed]
- 6. Kumar, N.; Roopa; Bhalla, V.; Kumar, M. Beyond zinc coordination: Bioimaging applications of Zn(II)-complexes. *Coord. Chem. Rev.* **2021**, 427, 213550. [CrossRef]
- 7. Li, T.; Schulz, S.; Roesky, P.W. Synthesis, Reactivity and Applications of Zinc–Zinc Bonded Complexes. *Chem. Soc. Rev.* **2012**, *41*, 3759–3771. [CrossRef]
- 8. Dumur, F. Zinc Complexes in OLEDs: An Overview. Synth. Met. 2014, 195, 241–251. [CrossRef]
- 9. Ho, K.-Y.; Yu, W.-Y.; Cheung, K.-K.; Che, C.-M. Blue luminescent zinc(II) complexes with polypyridylamine ligands: Crystal structures and luminescence properties. *J. Chem. Soc. Dalton Trans.* **1999**, *10*, 1581–1586. [CrossRef]
- 10. Wang, S. Luminescence and electroluminescence of Al (III), B (III), Be (II) and Zn (II) complexes with nitrogen donors. *Coord. Chem. Rev.* **2001**, 215, 79–98. [CrossRef]
- 11. Caruso, U.; Panunzi, B.; Roviello, A.; Tingoli, M.; Tuzi, A. Two Aminobenzothiazole Derivatives for Pd(II) and Zn(II) Coordination: Synthesis, Characterization and Solid State Fluorescence. *Inorg. Chem. Commun.* **2011**, *14*, 46–48. [CrossRef]
- 12. Gomes, C.S.B.; Gomes, P.T.; Duarte, M.T.; Di Paolo, R.E.; Maçanita, A.L.; Calhorda, M.J. Synthesis, Structure, and Photophysical Characterization of Blue-Green Luminescent Zinc Complexes Containing 2-Iminophenanthropyrrolyl Ligands. *Inorg. Chem.* 2009, 48, 11176–11186. [CrossRef]
- 13. Zheng, S.-L.; Chen, X.-M. Recent Advances in Luminescent Monomeric, Multinuclear, and Polymeric Zn(II) and Cd(II) Coordination Complexes. *Aust. J. Chem.* **2004**, *57*, 703–712. [CrossRef]
- 14. Yang, W.; Schmider, H.; Wu, Q.; Zhang, Y.; Wang, S. Syntheses, Structures, and Fluxionality of Blue Luminescent Zinc(II) Complexes: Zn(2,2',2"-tpa)Cl<sub>2</sub>, Zn(2,2',2"-tpa)<sub>2</sub>(O<sub>2</sub>CCF<sub>3</sub>)<sub>2</sub>, and Zn(2,2',3"-tpa)<sub>4</sub>(O<sub>2</sub>CCF<sub>3</sub>)<sub>2</sub> (tpa = Tripyridylamine). *Inorg. Chem.* **2000**, *39*, 2397–2404. [CrossRef] [PubMed]
- 15. Coles, M.P. Application of neutral amidines and guanidines in coordination chemistry. Dalton Trans. 2006, 8, 985–1001. [CrossRef]
- 16. Peak, D.A. 43. Diamidides. Part II. 2:4-Diaryltriazapentadienes. J. Chem. Soc. 1952, 1952, 215–226. [CrossRef]
- 17. Kopylovich, M.N.; Lasri, J.; Guedes da Silva, M.F.C.; Pombeiro, A.J.L. Single-pot template transformations of cyanopyridines on a PdII centre: Syntheses of ketoimine and 2,4-dipyridyl-1,3,5-triazapentadiene palladium(II) complexes and their catalytic activity for microwaveassisted Suzuki—Miyaura and Heck reactions. *Dalton Trans.* 2009, 16, 3074–3084. [CrossRef] [PubMed]
- 18. Leitch, A.A.; Korobkov, I.; Assoud, A.; Brusso, J.L. Noninnocent pyridyl nitrogens: Unprecedented interconversion of N-bridgehead-thiadiazolium salts and thiatriazine in the generation of thiatriazinyl. *Chem. Commun.* **2014**, *50*, 4934–4936. [CrossRef]
- 19. Castañeda, R.; Hollingshead, A.; Gabidullin, B.; Brusso, J.L. Probing the Coordination Chemistry of N-2-Pyridylimidoyl-2-pyridylamidine: A Versatile Ligand with Multiple Coordination Sites. *Cryst. Growth Des.* **2017**, *17*, 6572–6578. [CrossRef]
- Castañeda, R.; Harriman, K.L.M.; Wong, J.W.L.; Gabidullin, B.; Murugesu, M.; Brusso, J.L. Rational Design of Tetranuclear Complexes Employing N-Imidoylamidine Based Ligands. Eur. J. Inorg. Chem. 2019, 2019, 963–972. [CrossRef]
- 21. Castañeda, R.; Rouzières, M.; Clérac, R.; Brusso, J.L. Controlling the Nuclearity and Topology of Cobalt Complexes through Hydration at the Ppm Level. *J. Mater. Chem. C* **2020**, *8*, 4401–4407. [CrossRef]
- 22. Maddison, K. Exploring Square Planar Complexes of Copper and Nickel by Employing the N-2-Pyridylimidoyl-2-Pyridylamidine Ligand Framework; University of Ottawa: Ottawa, ON, Canada, 2018.
- 23. Kitos, A.A.; Gálico, D.A.; Castañeda, R.; Ovens, J.S.; Murugesu, M.; Brusso, J.L. Stark Sublevel-Based Thermometry with Tb(III) and Dy(III) Complexes Cosensitized via the 2-Amidinopyridine Ligand. *Inorg. Chem.* **2020**, *59*, 11061–11070. [CrossRef]
- Kitos, A.A.; Gálico, D.A.; Mavragani, N.; Castañeda, R.; Moilanen, J.O.; Brusso, J.L.; Murugesu, M. Probing Optical and Magnetic Properties via Subtle Stereoelectronic Effects in Mononuclear DyIII-Complexes. *Chem. Commun.* 2021, 57, 7818–7821. [CrossRef] [PubMed]
- 25. Safin, D.A.; Tumanov, N.A.; Leitch, A.A.; Brusso, J.L.; Filinchuk, Y.; Murugesu, M. Elucidating the Elusive Crystal Structure of 2,4,6-tris(2-pyrimidyl)-1,3,5-triazine (TPymT) through X-ray Powder Diffraction. *CrystEngComm* **2015**, 17, 2190–2195. [CrossRef]
- 26. Sheldrick, G.M. SADABS, Bruker/Siemens Area Detector Absorption Correction Program V.2.0.3; Bruker AXS: Madison, WI, USA, 2003.

27. Sheldrick, G.M. SHELXT — Integrated space-group and crystal-structure determination. *Acta Crystallogr. Sect. A Found. Adv.* **2015**, 71, 3–8. [CrossRef]

- 28. Sheldrick, G.M. Crystal structure refinement with SHELXL. *Acta Crystallogr. Sect. C Struct. Chem.* **2015**, *71*, 3–8. [CrossRef] [PubMed]
- 29. Groom, C.R.; Bruno, I.J.; Lightfoot, M.P.; Ward, S.C. The Cambridge Structural database. *Acta Crystallogr.* **2016**, *B72*, 171–179. [CrossRef]
- 30. Yang, L.; Powell, D.R.; Houser, R.P. Structural Variation in Copper(I) Complexes with Pyridylmethylamide Ligands: Structural Analysis with a New Four-Coordinate Geometry Index. *Dalton Trans.* **2007**, *9*, 955–964. [CrossRef]
- 31. Dubrawski, Z.; Heidebrecht, J.; Puerta Lombardi, B.M.; Hyla, A.S.; Willkomm, J.; Radford, C.L.; Lin, J.-B.; Welch, G.C.; Ponnurangam, S.; Roesler, R.; et al. Ligand-centered electrochemical processes enable CO<sub>2</sub> reduction with a nickel bis(triazapentadienyl) complex. *Sustain. Energy Fuels* **2019**, *3*, 1172. [CrossRef]
- 32. Kajiwara, T.; Kamiyama, A.; Ito, T. Complexed bridging ligand, {Cu(bptap)<sub>2</sub>}, as a ferromagnetic coupler. *Chem. Comm.* **2002**, 12, 1256. [CrossRef]
- 33. Addison, A.W.; Rao, T.N.; Reedijk, J.; van Rijn, J.; Verschoor, G.C. Synthesis, structure, and spectroscopic properties of copper(II) compounds containing nitrogen–sulphur donor ligands; the crystal and molecular structure of aqua[1,7-bis(*N*-methylbenzimidazol-2'-yl)-2,6-dithiaheptane]copper(II) perchlorate. *J. Chem. Soc. Dalton Trans.* **1984**, 7, 1349–1356. [CrossRef]
- 34. Dong, G.-H.; Xue, R.-D.; Li, J. Chlorido(pyridine-2-carboximidamide-κ2N1,N2)zinc(II) chloride dihydrate. *Acta Crystallogr. E Struct. Rep. Online* **2010**, *E66*, m1557. [CrossRef] [PubMed]

**Disclaimer/Publisher's Note:** The statements, opinions and data contained in all publications are solely those of the individual author(s) and contributor(s) and not of MDPI and/or the editor(s). MDPI and/or the editor(s) disclaim responsibility for any injury to people or property resulting from any ideas, methods, instructions or products referred to in the content.